Published in final edited form as:
Nitric Oxide. 2010 November 1; 23(3): 199–205. doi:10.1016/j.niox.2010.06.003.

Differential Roles of Nitric Oxide Synthases in Regulation of Ultraviolet B Light-induced Apoptosis

Wei Liu and **Shiyong Wu***
Department of Chemistry and Biochemistry, Edison Biotechnology Institute and Molecular and Cellular Biology Program, Ohio University, Athens, Ohio 45701

Abstract

Ultraviolet B light (UVB) activates nitric oxide synthase(s) (NOS) and nitric oxide ($NO^{\bullet}$) production, which plays a role in regulation of apoptosis. However the role of $NO^{\bullet}$ in UVB-induced apoptosis remains controversial. In this study, we analyzed expression and activation of constitutive NOSs (cNOSs) and their roles in UV-induced apoptosis of HaCaT keratinocytes. Our data showed that the expression of neuronal NOS (nNOS) was increased while endothelial NOS (eNOS) was uncoupled in the early phase (0–6 h) post-UVB. The expression of both cNOSs peaked at 12 h post-UVB and $NO^{\bullet}$ was transiently elevated with 30 min and then steadily rose from 6–18 h post-UVB. The expression of iNOS was detected at 6 h post-UVB and then sturdily increased. Inhibition of cNOSs with L-NAME reduced the inducibility of $NO^{\bullet}$ in the early and late phases of irradiation. Along with the eNOS uncoupling, an increased level of peroxynitrite ($ONOO^{-}$) was detected in the early phase, but not in the late phase post-UVB. Inhibition of cNOSs reduced the production of $ONOO^{-}$ in the early time, but led to an increase of $ONOO^{-}$ in the late time after UVB-irradiation. The results indicate that cNOSs regulate $NO^{\bullet}/ONOO^{-}$ imbalance after UVB-irradiation. Our data suggested that the activation of cNOSs in the early phase post-UVB leads to $NO^{\bullet}/ONOO^{-}$ imbalance and promotes apoptosis via a caspase 3-independent pathway. The elevation of $NO^{\bullet}$ in the late phase of UVB-irradiation is mainly produced by inducible NOS (iNOS). However, cNOSs also contribute to the $NO^{\bullet}$ production and to maintain a higher $NO^{\bullet}/ONOO^{-}$ ratio, which reduces caspase 3 activity and protects cells from UVB-induced apoptosis.

Keywords

UVB; cNOS; nitric oxide; caspase 3 and apoptosis

Introduction

UVB-induced $NO^{\bullet}$ production occurs in a dose- and time-dependent manner. In human keratinocytes, the UVB-dose-dependent induction of $NO^{\bullet}$ reaches a maximal $NO^{\bullet}$ release of 3-fold with a treatment of 120 mJ/cm^2 UVB. Higher doses of UVB result in similar increases in generation of $NO^{\bullet}$ [1–3]. UVB induces a rapid elevation of $NO^{\bullet}$, which is recorded at 20 sec and reaches a peak at 40 sec in keratinocytes [4]. A maximal prolonged

*To whom all correspondence should be addressed. Edison Biotechnology Institute and Department of Chemistry and Biochemistry, Ohio University, Athens, OH 45701, Phone: 740-597-1318, Fax: 740-593-4795, wus1@ohio.edu.

$NO^{\bullet}$ production occurs between 17 and 48 hours post UVB-irradiation based on cell type [5,6]. Keratinocytes were shown to contain nNOS (NOS1), iNOS (NOS2) and eNOS (NOS3), the three members of NOS family [7–9]. UVB-activated NOSs generate $NO^{\bullet}$ from L-arginine (L-Arg). Since [L-Arg] is low in cells, rapid consumption of L-Arg results in a L-Arg depletion, which leads to cNOS uncoupling and increases production of $O_2^{\bullet -}$ [4,10,11]. $NO^{\bullet}$ is able to rapidly react with $O_2^{\bullet -}$ to from $ONOO^-$, which is a powerful oxidant [12,13].

An elevated cytosolic [$NO^{\bullet}$] could have anti- or pro-apoptotic effect on keratinocytes upon UVB-irradiation [14–16]. Superoxide was suggested to play a role in regulation of nitric oxide-mediated anti-or pro-apoptosis after the irradiation [16]. However it is not clear how these NOSs were involved in the regulation of UV-induced apoptosis in a contrasting manner. Our recent reports suggested that the UVB-induced activation of constitutive NOS (cNOS), including nNOS and eNOS, in combination of oxidative stress, promoted apoptosis of keratinocytes [4,17]. In this report, we further elucidate the mechanism for coordinative regulation of apoptosis of keratinocytes by the three NOSs after UVB-irradiation. Our date suggested that cNOSs are the key contributors for a transient elevation of $NO^{\bullet}$ and $ONOO^-$ in the early phase post-UVB, while iNOS is a major contributor for $NO^{\bullet}$ production in the late phase post-UVB. However, cNOSs also generated $NO^{\bullet}$ and play a role in maintaining a healthier $NO^{\bullet}/ONOO^-$ ratio in the late phase of UVB-irradiation.

Materials and Methods

Cell Culture

All chemicals were obtained from Sigma (St. Louis, MO), unless otherwise mentioned. The HaCat cells (human keratinocyte cell line, kindly provided by Dr. Nihal Ahmad, University of Wisconsin, Madison, WI) were cultured in 100 mm^2 cell culture plates in Dulbecco's modification of eagle's medium (DMEM, Mediatech, Manassas, VA) with 10% (v/v) fetal bovine serum (FBS, Hyclone, Waltham, MA). Penicillin and streptomycin were added to the culture medium, and the cells were incubated at 37°C and 5% CO_2.

Ultraviolet irradiation

Two UVB lamps (UVP, Upland, CA) were measured by a UVP model UVX digital radiometer (UVP, Upland, CA) after the lamps warmed up for 5 min. The cell culture medium was replaced with 1 mL/plate phosphate buffered saline (PBS) and then the cells were irradiated with a total dose of 75 mJ/cm^2, which is in the rage of 1 minimal erythema dose (MED) for human [18]. After UVB-irradiation, fresh medium was added to the culture plates and the cells were returned to the incubator for further research.

Cell treatments

L-N^G-nitro-arginine methyl ester (L-NAME) [19] was added to HaCat cells to a final concentration of 1 mM at 6 h before UVB-irradiation. After irradiation, the cells were continuously treated with L-NAME (1 mM) for a short or prolonged period of time. For the short treatment, the cells were incubated with the medium containing L-NAME for 0.5 h post-irradiation. Then the medium was replaced with fresh medium without L-NAME and the cells were incubated for another 17.5 h. For prolonged treatment, the cells were incubated with the medium containing L-NAME for a continuous 18 h.

Nitric oxide and peroxynitrite assay

The concentration of $NO^{\bullet}$ or $ONOO^-$ was measured by a standard nitric oxide synthase assay [20] kit (Sigma, St. Louis, MO). The cells were placed in a 96-well plate. After treatment, the medium was removed. Then 190 μL reaction buffer, 10 μL L-arginine (1 mM) and 0.1 μL 4,5-diaminofluorescein diacetate (DAF-2DA, for $NO^{\bullet}$) (5 mM) or

diaminorhodamine (DAR, for $ONOO^-$) (5 mM) were added to each well. The cells were incubated for 2 h in dark at room temperature and the fluorescence was read by SpectraMax M2 fluorescence plate reader (Molecular Devices, Sunnyvale, CA) at ex490/em520 nm for DAF-2DA or ex 488/em 515 nm for DAR.

Cell viability was determined by Thiazolyl Blue Tetrazolium Bromide (MTT) assay [21]. 0.01 mL MTT solution (5 mg/mL, Millipore, Billerica, MA) was added into 96-well plate after nitric oxide and peroxynitrite assay. Then the plate was incubated at 37°C for 4 h and 0.1 mL isopropanol with 0.04 M HCl was added to each well. The absorbance of MTT solution was measured by optical reader at 570 nm. The fluorescence intensity of DAF-2DA and DAR was corrected by diving by the cell viability.

$$\text{Corrected Fluorescence Intensity} = (\text{Fluorescence Intensity})/(\text{Cell viability})$$

Caspase-3 activity assay

Cells were cultured in 100 mm plates. At 18 h post-UVB, cells were harvested by trypsin and rinsed in cold PBS twice. Then cells lysates were prepared in lysis buffer (200 mM Tris, pH 7.5, 2 M NaCl, 20 mM EDTA, 0.2% Triton X-100) by sonication. Same amount of proteins (200 μg) from each sample were diluted to 300 μL with the same lysis buffer in a 96-well plate and the substrate of caspase-3 FAM-DEVD-FMK [22] (10 μL, Cell Technology, Mountain View, CA) was added into each sample. After 1 h incubation at 37°C in the dark, the fluorescence intensity was measured by SpectraMax M2 fluorescence plate reader (Molecular Devices, Sunnyvale, CA) at ex488nm/em515nm.

Apoptosis assay

The apoptotic cell death was analyzed by determination of the loss of membrane phospholipid symmetry and membrane integrity [23] using a fluorescein isothiocyanate (FITC) conjugated-annexin V (ANX5)/propidium iodide (PI) apoptosis detection kit (BD Biosciences, Franklin Lakes, NJ) following the manufacturer's protocol. Briefly, the cells were harvested by 0.05% trypsin digestion, combined with the cells floating in the medium and washed twice with cold PBS. The cells were then suspended in annexin V binding buffer (10 mM Hepes/NaOH, pH 7.4, 140 mM NaCl and 2.5 mM $CaCl_2$) at 10^6 cells/mL. 100 μL of the cell suspension was mixed with 5 μL ANX5-FITC and 5 μL PI. The cell mixture was incubated in dark for 15 min and the ANX5/PI double-stained cells were analyzed by using a FACSort Flow Cytometer (BD science, Franklin Lakes, NJ) equipped with CellQuest software (BD science, Franklin Lakes, NJ). A minimum of 1×10^4 cells was used for each analysis and cell debris is excluded by appropriate forward light scatter threshold setting. The numbers of cells positive for both ANX5 and PI were counted. The relative percentage change of apoptotic cells (relative %AC) was calculated as:

$$\text{Relative \%AC} = [\%\text{AC (+UV)} - \%\text{AC (+UV+LNAME)}]/[\%\text{AC (+UV)}]$$

Western blot analysis

The antibodies against nNOS, eNOS, iNOS, caspase-3 and mouse IgG were purchased from Santa Cruz Biotechnology (Santa Cruz, CA). The anti-PARP was purchased from Cell Signaling (Danvers, MA). The anti-β-actin was purchased from Sigma (St. Louis, MO) and anti-rabbit IgG was from BioRad (Hercules, CA). The monomers and dimers of cNOSs were analyzed on a low-temperature, SDS-resistant SDS-PAGE [24]. Briefly, the cells were lysed after treatment in NP-40 lysis buffer (2% NP-40, 80 mM NaCl, 100 mM Tris-HCl, 0.1% SDS) containing a Proteinase Inhibitor Cocktail (Complete™, Roche Molecular

Biochemicals, Indiana, IN). Then the protein samples were added to five-fold Laemmli buffer (0.32 M Tris-HCl, pH 6.8, 0.5 M glycine, 10% SDS, 50% glycerol, and 0.03% bromophenol blue) without boiling. These proteins were separated on SDS-PAGE with reducing gel (with 2.5% 2-mercaptoethanol) at 4°C before transferred onto a nitrocellulose membrane. Caspase 3 and PARP were analyzed on regular SDS-PAGE. The proteins were boiled in the loading buffer and separated on SDS-PAGE at room temperature before transferred onto a nitrocellulose membrane. The membrane was blocked with 5% (w/v) skim milk in TBST (20 mM Tris-HCl, pH 7.5, 150 mM NaCl, 0.1% Tween 20) for 1 h and then incubated with corresponding antibodies at 4°C overnight. After washing with TBST, the membrane was incubated with HRP–conjugated anti-rabbit antibody for 1 h at room temperature. Membranes were washed three times in TBST, two times in TBS, and developed in West Pico Supersignal chemiluminescent substrate (Pierce, Rockford, IL).

Statistics

All values shown in figures were mean±SE. Independent Student's *t-test* was used to analyze the statistic significance of data before normalization and applied to compare every two groups. 95% confidence interval ($p<0.05$) was used to denote the statistical significance.

RESULTS

Time-dependent analysis of cNOSs expression and uncoupling after UVB-irradiation

To analyze the roles of cNOSs in UVB-induced apoptosis, we first determined the effects of UVB irradiation on expression and coupling of eNOS and nNOS in human keratinocytes (HaCat). The cNOS uncoupling was detected by low-temperature SDS-resistant SDS-PAGE as previously reported [24]. Both nNOS and eNOS were detected in dimerized and monomerized forms in HaCaT cells (Fig. 1A and 1B). After UVB treatment (75 mJ/cm^2), the expression of nNOS was increased shortly after the irradiation and peaked at 12 h post-UVB. The ratio between dimer and monomer of nNOS was not changed in the first half hour after UVB indicating that the newly synthesized nNOS formed both dimers and monomers (Fig. 1A). In contrast to nNOS, the expression of eNOS was not significantly changed until 12 h after UVB treatment (Fig. 1B). However, the ratio between dimer and monomer of eNOS was rapidly reduced with a shift from dimers to monomers (Fig. 1B). The expression of iNOS was detected at 6 h post-UVB and then continuously increased during the whole period of measurement (Fig. 1C).

The contribution of cNOS in UVB-induced elevation of $NO^{\bullet}$ and $ONOO^{-}$

To determine the contribution of cNOS in generating $NO^{\bullet}$ and oxidative stress after UVB-irradiation, we measured the time-dependent production of $NO^{\bullet}$ and $ONOO^{-}$ in the presence and absence of the selective cNOS inhibitor L-NAME [19] using specific fluorescent dyes. Our data showed that the production of $NO^{\bullet}$ increased immediately and generated the first peak, which was approximately 2 times that of the background level, at 10 min after UVB-irradiation (Fig. 2A, Table I). The production of $NO^{\bullet}$ was reduced and remained low for 6 h and then raised to approximately 10 times of the background level at 18 h post-UVB and remained high (Fig. 2A, Table I). The UVB-induced immediate elevation of $NO^{\bullet}$ was significantly inhibited by L-NAME (Fig. 2B, Table I). However, the later elevation of $NO^{\bullet}$ was only reduced slightly by L-NAME (Fig. 2B, Table I). These results suggested that the early elevation of $NO^{\bullet}$ was depended on the activation cNOS upon UVB-irradiation. The UVB-induced late elevation of $NO^{\bullet}$ was largely depended on the increased expression of iNOS, but cNOSs also made a contribution since $NO^{\bullet}$ levels were partially reduced by L-NAME.

The UVB-induced production of $ONOO^-$ also increased immediately and peaked at approximately 1.5-fold of the background level at 5 min post-irradiation. The production of $ONOO^-$ was reduced and remained low without statistically significant change during the whole experiment (Fig. 2C, Table I). The UVB-induced immediate elevation of $ONOO^-$ was also significantly inhibited by L-NAME, while $ONOO^-$ was only slightly decreased in the late stage of irradiation upon treating with L-NAME (Fig. 2D, Table I). These results suggested that the UVB-induced uncoupling of cNOS could be a source of generating $O_2^{\bullet -}$, and sequentially $ONOO^-$ as we previously reported [4,10]. However, cNOS was also contributed to the reduction of oxidative stress and therefore the production of $ONOO^-$ at late stage of UVB-irradiation.

The roles of NOSs in regulation of UVB-induced caspase 3 activation and apoptosis

The role of $NO^{\bullet}$ in regulation of apoptosis is controversial [14–16,25–28]. Our recently studies suggested that early activation of NOSs promotes apoptotic death of keratinocytes upon UVB-irradiation [4,17]. To further analyze the roles of NOSs in regulation of UVB-induced apoptosis of keratinocytes, we determined the extent of effects of a short or prolonged inhibition of cNOS on UVB-induced caspase 3 activation and apoptosis. Our data showed that while the short incubation of L-NAME after UVB-irradiation did not statistically significantly affect caspase 3 activity, the prolonged incubation of L-NAME increased caspase 3 activity by 55±3% (Fig. 3A). Either short or prolonged incubation of L-NAME did not statistically significantly affect caspase 3 activity in the absence of UVB-irradiation (Fig. 3A). Our data also showed that the increased caspase 3 activity after prolonged treatment of L-NAME was not a result of an elevation of p20, the active form of caspase 3 (Fig. 3B).

To confirm that the caspase 3 activity was increased without changing the amount of the p20 after prolonged incubation of L-NAME, we determined the cleavage of PARP, a caspase 3 substrate. Our data showed that the cleavage of PARP was increased with the prolonged inhibition of cNOS after UVB-irradiation (Fig. 4, Lane 6 vs. 2 and 4). The cleavage of PARP was not affected by L-NAME alone without the irradiation or a short incubation of L-NAME after UVB-irradiation (Fig. 4, Lane 3,5 vs. 1 and Lane 4 vs. 2). These results suggest that the combination effect of higher $[NO^{\bullet}]$ with lower $[ONOO^-]$ in the late phase of UVB-irradiation (Table I) may lower the net amount of the active form of caspase 3.

Last we determined the role of cNOS in UVB-induced apoptosis of keratinocytes. After the short period of inhibition of cNOS, the amount of UVB-induced apoptotic cells were reduced by 7.3%, which was a relative 24.2% reduction (Fig. 5). In contrast, the prolonged inhibition of cNOS increased the amount of UVB-induced apoptotic cells by 3.6%, which was a relative 11.9% increase (Fig. 5). These results suggest that the effect of cNOS on UVB-induced apoptosis is via a caspase 3-independed pathway during the early period and a caspase 3-depended pathway in the late period of irradiation.

Discussion

UVB-irradiation activates both extrinsic and intrinsic apoptotic pathways [29]. With the extrinsic pathway, UVB induces the aggregation of Fas receptors, which recruits FADD and activates caspase 8 [30,31]. With the intrinsic pathway, UVB induces reactive oxygen species (ROS) production, which leads to mitochondrial cytochrome *c* (*cyto c*) release and caspase 9 activation [32,33]. Both caspase 8 and 9 activate caspase 3, which catalyzes the specific cleavage and activation of many key apoptosis-related proteins [34]. UVB also activates a caspase-independent, p38 mitogen-activated protein kinase (MAPK)-induced *cyto c*-mediated pathway in promoting apoptosis [35]. The UVB-induced NOSs activation and $NO^{\bullet}$ release play roles in regulation of apoptosis. An elevation of $NO^{\bullet}$ could promote

apoptosis through the formation of more reactive oxidative species such as $ONOO^-$, which induces oxidative protein modifications including oxidation or nitration of various amino acid residues, such as methionine and tyrosine [36,37]. However, high levels of $NO^\bullet$ could also inhibit apoptosis by s-nitrosylation of caspases [38].

After UVB-irradiation, the activation of NOSs and production of $NO^\bullet$ have been shown to be pro- and anti-apoptotic [14–16,25–28]. Our recent reports suggested that UVB-induced early activation of cNOS leads to the uncoupling of cNOS and elevation of $O_2^{\bullet-}$, which reacts with $NO^\bullet$ to form $ONOO^-$ and promotes apoptosis due to a $NO^\bullet/ONOO^-$ imbalance [4,10,17]. In this study, we demonstrated that in the early phase of UVB-irradiation, rapid transitional elevations of $NO^\bullet$ and $ONOO^-$ were mainly dependent on the activation of cNOSs. Inhibition of cNOSs by L-NAME significantly reduced the inducibility of $NO^\bullet$ and $ONOO^-$ productions after the irradiation (Fig. 2, Panel B vs. A; Panel D vs. C; Table I). The production of $ONOO^-$ peaks ahead of $NO^\bullet$, which agreed with our previous report [4]. The UVB-induced up-regulation of nNOS expression was paired in monomers (uncoupled form) and dimers (coupled form) (Fig. 1A, Lanes 1–4). In contrast, the eNOS expression after UVB-irradiation was more in monomer than in dimer. Further more, UVB appears to reduce the dimer and the dimer/monomer ratio of eNOS (Fig. 1B, Lanes 3–5 vs. 1,2). Since the uncoupled eNOS generates $O_2^{\bullet-}$ and therefore $ONOO^-$ [12], our results suggest that uncoupled eNOS is likely a source for UVB-induced oxidative stress. The inhibition of cNOSs activation at the early phase of the irradiation reduced the apoptotic death of the irradiated keratinocytes (Fig. 5, ST vs. No Treat), which agreed with our previous report [4]. Interestingly, the reduction of apoptosis was not accompanied with a reduced activity of caspase 3 (Figs. 3,4, ST vs. No Treat), which is one of the major players in UVB-induced apoptosis [39,40]. The results indicated that the UVB-induced and cNOS-mediated early signaling for inducing apoptosis is via a caspase 3-independent pathway.

In the late phase of UVB-irradiation, the $NO^\bullet$ production is contributed to by both cNOS and iNOS [1,2,41–43]. Our data showed that the expressions of all three NOSs were significantly increased in the late phase of the irradiation (Fig. 1). The increased expressed cNOSs existed mainly as dimers, which increased the ratio of dimer/monomer (Fig. 1A, 1B). The UVB-induced production of $NO^\bullet$ was dramatically elevated from 6– 24 h post-UVB, while the $ONOO^-$ level was not statistically changed during the same period (Figs. 2A and 2C;Table I). The inhibition of cNOS reduced $NO^\bullet$ production by approximately 10–20% at 18 to 24 h post-UVB (Fig. 2A vs. 2B;Table I) suggesting that the iNOS, whose expression was induced during the period after UVB (Fig. 1C) [44], is a key contributor of $NO^\bullet$ production during this period. Interestingly, with the inhibition of cNOS, the $ONOO^-$ production was steadily increased from 6–24 h post-UVB (Fig. 2D;Table I). These results indicate that cNOSs do not only contribute to $NO^\bullet$ production but also to reduce $ONOO^-$, and therefore maintain a healthier balance of $NO^\bullet/ONOO^-$ ratio, in the late phase of UVB-irradiation. This conclusion agrees with our observation that inhibition of cNOSs promotes apoptosis with an increased activity of caspase 3 and cleavage of PARP after UVB-irradiation (Figs. 3A and 4, LT vs. No Treat). The increased activity of caspase 3 was not correlated to an increased amount of activated caspase 3 (Fig. 3B), indicating that the bioavailability of $NO^\bullet$ may direct inhibit activated caspase 3 activity as previously reported [38].

Based on our results, we propose a signaling network for UVB-induced and NOSs-mediated apoptosis (Fig. 6). The UVB-induced expression of nNOS and uncoupling of eNOS are the main sources of $NO^\bullet$ and $ONOO^-$ productions in the early phase of UVB-irradiation. The elevation of $NO^\bullet/ONOO^-$ promotes apoptosis via a caspase 3-independent pathway. The elevation of $NO^\bullet$ in the late phase of UVB-irradiation is mainly produced by iNOS. However, cNOSs also contribute to the $NO^\bullet$ production and to maintain a higher $NO^\bullet$/

$ONOO^-$ ratio, which reduces caspase 3 activity and protects cells from UVB-induced apoptosis.

Supplementary Material

Refer to Web version on PubMed Central for supplementary material.

Acknowledgments

We thank Ms. Lei Wang for her assistance in analysis of apoptosis using the flow cytometer. We thank Mr. Oliver L. Carpenter for editorial assistance. This work is supported by 2R56CA086928 (to S. W.) and 2RO1CA086928 (to S. W.).

References

1. Deliconstantinos G, Villiotou V, Stravrides JC. Release by ultraviolet B (u.v.B) radiation of nitric oxide (NO) from human keratinocytes: a potential role for nitric oxide in erythema production. Br J Pharmacol 1995;114:1257–1265. [PubMed: 7620717]
2. Deliconstantinos G, Villiotou V, Stavrides JC. Nitric oxide and peroxynitrite released by ultraviolet B-irradiated human endothelial cells are possibly involved in skin erythema and inflammation. Exp Physiol 1996;81:1021–1033. [PubMed: 8960707]
3. Deliconstantinos G, Villiotou V, Stavrides JC. Alterations of nitric oxide synthase and xanthine oxidase activities of human keratinocytes by ultraviolet B radiation. Potential role for peroxynitrite in skin inflammation. Biochemical Pharmacology 1996;51:1727–1738. [PubMed: 8687488]
4. Wu S, Wang L, Jacoby AM, Jasinski K, Kubant R, Malinski T. Ultraviolet B Light-induced Nitric Oxide/Peroxynitrite Imbalance in Keratinocytes-Implications for Apoptosis and Necrosis. Photochem Photobiol.
5. Gonzalez Maglio DH, Paz ML, Ferrari A, Weill FS, Czerniczyniec A, Leoni J, Bustamante J. Skin damage and mitochondrial dysfunction after acute ultraviolet B irradiation: relationship with nitric oxide production. Photodermatol Photoimmunol Photomed 2005;21:311–317. [PubMed: 16313242]
6. Seo SJ, Choi HG, Chung HJ, Hong CK. Time course of expression of mRNA of inducible nitric oxide synthase and generation of nitric oxide by ultraviolet B in keratinocyte cell lines. Br J Dermatol 2002;147:655–662. [PubMed: 12366409]
7. Boissel JP, Ohly D, Bros M, Godtel-Armbrust U, Forstermann U, Frank S. The neuronal nitric oxide synthase is upregulated in mouse skin repair and in response to epidermal growth factor in human HaCaT keratinocytes. J Invest Dermatol 2004;123:132–139. [PubMed: 15191553]
8. Nakai K, Kubota Y, Kosaka H. Inhibition of nuclear factor kappa B activation and inducible nitric oxide synthase transcription by prolonged exposure to high glucose in the human keratinocyte cell line HaCaT. Br J Dermatol 2004;150:640–646. [PubMed: 15099358]
9. Nakai K, Fujii S, Yamamoto A, Igarashi J, Kubota Y, Kosaka H. Effects of high glucose on NO synthesis in human keratinocyte cell line (HaCaT). J Dermatol Sci 2003;31:211–218. [PubMed: 12727025]
10. Lu W, Laszlo CF, Miao Z, Chen H, Wu S. The role of nitric-oxide synthase in the regulation of UVB light-induced phosphorylation of the alpha subunit of eukaryotic initiation factor 2. The Journal Of Biological Chemistry 2009;284:24281–24288. [PubMed: 19586904]
11. Huk I, Nanobashvili J, Neumayer C, Punz A, Mueller M, Afkhampour K, Mittlboeck M, Losert U, Polterauer P, Roth E, Patton S, Malinski T. L-arginine treatment alters the kinetics of nitric oxide and superoxide release and reduces ischemia/reperfusion injury in skeletal muscle. Circulation 1997;96:667–675. [PubMed: 9244241]
12. Kalinowski L, Malinski T. Endothelial NADH/NADPH-dependent enzymatic sources of superoxide production: relationship to endothelial dysfunction. Acta Biochim Pol 2004;51:459–469. [PubMed: 15218542]
13. Padmaja S, Huie RE. The reaction of nitric oxide with organic peroxyl radicals. Biochem Biophys Res Commun 1993;195:539–544. [PubMed: 8373394]

14. Weller R, Schwentker A, Billiar TR, Vodovotz Y. Autologous nitric oxide protects mouse and human keratinocytes from ultraviolet B radiation-induced apoptosis. Am J Physiol Cell Physiol 2003;284:C1140–C1148. [PubMed: 12676653]
15. Yamaoka J, Kawana S, Miyachi Y. Nitric oxide inhibits ultraviolet B-induced murine keratinocyte apoptosis by regulating apoptotic signaling cascades. Free Radical Research 2004;38:943–950. [PubMed: 15621712]
16. Weller R, Billiar T, Vodovotz Y. Pro- and anti-apoptotic effects of nitric oxide in irradiated keratinocytes: the role of superoxide. Skin Pharmacol Appl Skin Physiol 2002;15:348–352. [PubMed: 12239430]
17. Wang L, Liu W, Parker SH, Wu S. Nitric oxide synthase activation and oxidative stress, but not intracellular zinc dyshomeostasis, regulate ultraviolet B light-induced apoptosis. Life Sci 86:448–454. [PubMed: 20149802]
18. Placzek M, Gaube S, Kerkmann U, Gilbertz KP, Herzinger T, Haen E, Przybilla B. Ultraviolet B-induced DNA damage in human epidermis is modified by the antioxidants ascorbic acid and D-alpha-tocopherol. J Invest Dermatol 2005;124:304–307. [PubMed: 15675947]
19. Boer R, Ulrich WR, Klein T, Mirau B, Haas S, Baur I. The inhibitory potency and selectivity of arginine substrate site nitric-oxide synthase inhibitors is solely determined by their affinity toward the different isoenzymes. Mol Pharmacol 2000;58:1026–1034. [PubMed: 11040050]
20. Marletta MA, Hurshman AR, Rusche KM. Catalysis by nitric oxide synthase. Curr Opin Chem Biol 1998;2:656–663. [PubMed: 9818193]
21. Boethling RS, Weaver TL. A new assay for diaphorase activity in reagent formulations, based on the reduction of thiazolyl blue. Clin Chem 1979;25:2040–2042. [PubMed: 41650]
22. Kuzelova K, Grebenova D, Hrkal Z. Labeling of apoptotic JURL-MK1 cells by fluorescent caspase-3 inhibitor FAM-DEVD-fmk occurs mainly at site(s) different from caspase-3 active site. Cytometry A 2007;71:605–611. [PubMed: 17549763]
23. Schindl A, Klosner G, Honigsmann H, Jori G, Calzavara-Pinton PC, Trautinger F. Flow cytometric quantification of UV-induced cell death in a human squamous cell carcinoma-derived cell line: dose and kinetic studies. Journal Of Photochemistry And Photobiology. B, Biology 1998;44:97–106.
24. Zou MH, Shi C, Cohen RA. Oxidation of the zinc-thiolate complex and uncoupling of endothelial nitric oxide synthase by peroxynitrite. The Journal Of Clinical Investigation 2002;109:817–826. [PubMed: 11901190]
25. Fukunaga-Takenaka R, Fukunaga K, Tatemichi M, Ohshima H. Nitric oxide prevents UV-induced phosphorylation of the p53 tumor-suppressor protein at serine 46: a possible role in inhibition of apoptosis. Biochem Biophys Res Commun 2003;308:966–974. [PubMed: 12927814]
26. Schneiderhan N, Budde A, Zhang Y, Brune B. Nitric oxide induces phosphorylation of p53 and impairs nuclear export. Oncogene 2003;22:2857–2868. [PubMed: 12771937]
27. Suschek CV, Briviba K, Bruch-Gerharz D, Sies H, Kroncke KD, Kolb-Bachofen V. Even after UVA-exposure will nitric oxide protect cells from reactive oxygen intermediate-mediated apoptosis and necrosis. Cell Death Differ 2001;8:515–527. [PubMed: 11423912]
28. Suschek CV, Krischel V, Bruch-Gerharz D, Berendji D, Krutmann J, Kroncke KD, Kolb-Bachofen V. Nitric oxide fully protects against UVA-induced apoptosis in tight correlation with Bcl-2 up-regulation. J Biol Chem 1999;274:6130–6137. [PubMed: 10037696]
29. Takasawa R, Nakamura H, Mori T, Tanuma S. Differential apoptotic pathways in human keratinocyte HaCaT cells exposed to UVB and UVC. Apoptosis 2005;10:1121–1130. [PubMed: 16151645]
30. Bang B, Gniadecki R, Larsen JK, Baadsgaard O, Skov L. In vivo UVB irradiation induces clustering of Fas (CD95) on human epidermal cells. Exp Dermatol 2003;12:791–798. [PubMed: 14714559]
31. Elyassaki W, Wu S. Lipid rafts mediate ultraviolet light-induced Fas aggregation in M624 melanoma cells. Photochem Photobiol 2006;82:787–792. [PubMed: 16438619]
32. Pan MH, Hsieh MC, Kuo JM, Lai CS, Wu H, Sang S, Ho CT. 6-Shogaol induces apoptosis in human colorectal carcinoma cells via ROS production, caspase activation, and GADD 153 expression. Mol Nutr Food Res 2008;52:527–537. [PubMed: 18384088]

33. Paz ML, Gonzalez Maglio DH, Weill FS, Bustamante J, Leoni J. Mitochondrial dysfunction and cellular stress progression after ultraviolet B irradiation in human keratinocytes. Photodermatol Photoimmunol Photomed 2008;24:115–122. [PubMed: 18477129]
34. Claerhout S, Van Laethem A, Agostinis P, Garmyn M. Pathways involved in sunburn cell formation: deregulation in skin cancer. Photochem Photobiol Sci 2006;5:199–207. [PubMed: 16465306]
35. Assefa Z, Vantieghem A, Garmyn M, Declercq W, Vandenabeele P, Vandenheede JR, Bouillon R, Merlevede W, Agostinis P. p38 mitogen-activated protein kinase regulates a novel, caspase-independent pathway for the mitochondrial cytochrome c release in ultraviolet B radiation-induced apoptosis. J Biol Chem 2000;275:21416–21421. [PubMed: 10748072]
36. Kuhn DM, Aretha CW, Geddes TJ. Peroxynitrite inactivation of tyrosine hydroxylase: mediation by sulfhydryl oxidation, not tyrosine nitration. J Neurosci 1999;19:10289–10294. [PubMed: 10575026]
37. Zhang H, Joseph J, Feix J, Hogg N, Kalyanaraman B. Nitration and oxidation of a hydrophobic tyrosine probe by peroxynitrite in membranes: comparison with nitration and oxidation of tyrosine by peroxynitrite in aqueous solution. Biochemistry 2001;40:7675–7686. [PubMed: 11412121]
38. Bonavida B, Khineche S, Huerta-Yepez S, Garban H. Therapeutic potential of nitric oxide in cancer. Drug Resist Updat 2006;9:157–173. [PubMed: 16822706]
39. Liu S, Mizu H, Yamauchi H. Molecular response to phototoxic stress of UVB-irradiated ketoprofen through arresting cell cycle in G2/M phase and inducing apoptosis. Biochem Biophys Res Commun 2007;364:650–655. [PubMed: 17964538]
40. Anand S, Chakrabarti E, Kawamura H, Taylor CR, Maytin EV. Ultraviolet light (UVB and UVA) induces the damage-responsive transcription factor CHOP/gadd153 in murine and human epidermis: evidence for a mechanism specific to intact skin. J Invest Dermatol 2005;125:323–333. [PubMed: 16098044]
41. Deliconstantinos G, Villiotou V, Stavrides JC. Increase of particulate nitric oxide synthase activity and peroxynitrite synthesis in UVB-irradiated keratinocyte membranes. The Biochemical Journal 1996;320(Pt 3):997–1003. [PubMed: 9003391]
42. Kim JH, Hong Y, Shim CS. Mechanism of UV light-induced photorelaxation in isolated rat aorta. J Vet Sci 2000;1:81–86. [PubMed: 14614302]
43. Chen YC, Shen SC, Lee WR, Lin HY, Ko CH, Lee TJ. Nitric oxide and prostaglandin E2 participate in lipopolysaccharide/interferon-gamma-induced heme oxygenase 1 and prevent RAW264.7 macrophages from UV-irradiation-induced cell death. J Cell Biochem 2002;86:331–339. [PubMed: 12112002]
44. Chang HR, Tsao DA, Wang SR, Yu HS. Expression of nitric oxide synthases in keratinocytes after UVB irradiation. Arch Dermatol Res 2003;295:293–296. [PubMed: 14615895]

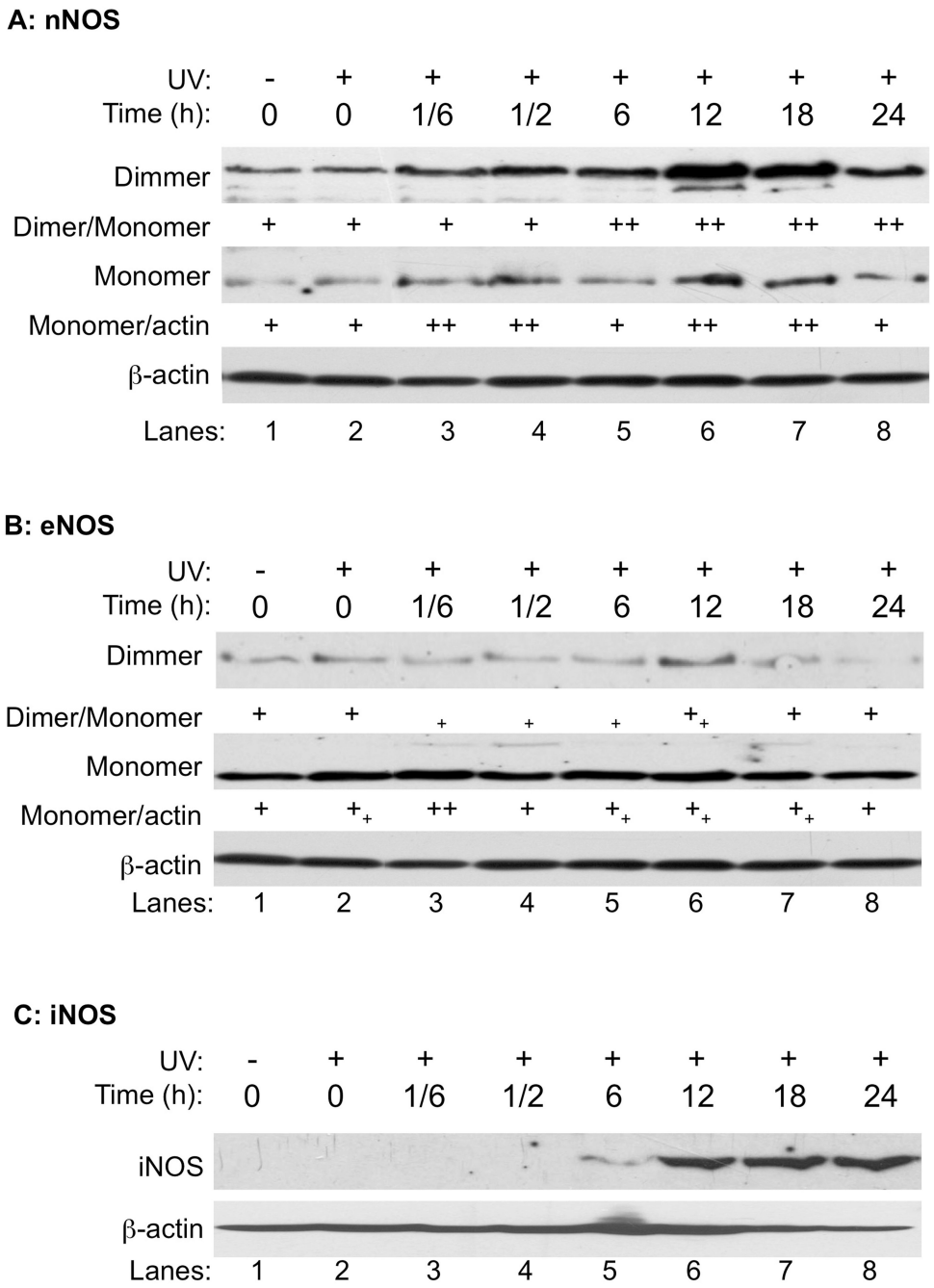

Fig. 1.

The effect of UVB on cNOSs expression and dimerization. HaCaT cells were UVB-irradiated (75 mJ/cm^2) and harvested at different time-points as indicated. The monomers and dimers of cNOSs were separated on a low-temperature SDS-resistant SDS-PAGE and the iNOS expression was determined by regular western blotting. The levels of β-actin were also probed as a loading control. Panel A: nNOS. Panel B: eNOS. Panel C: iNOS. The intensities of the protein bands were semi-quantitated by ImageJ (Version 1.42k, NIH). +: No change; ++: Increased >50%; $+_+$: Increased <50%; $_+$: Decreased <50%.

A. NO• production

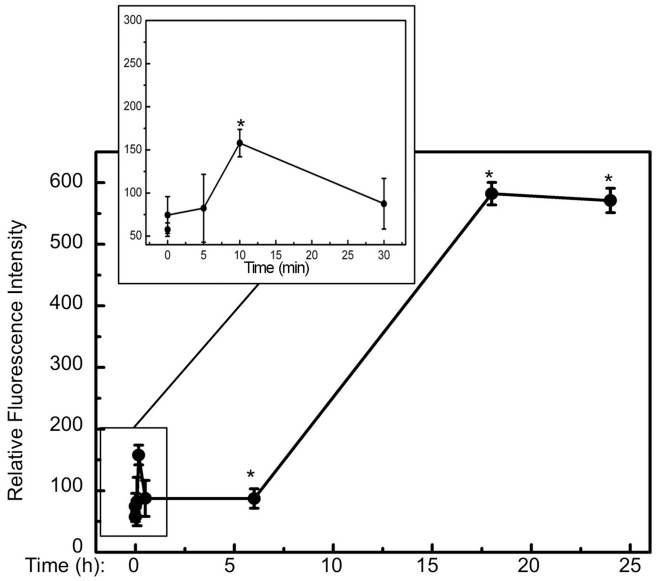

B. NO• production in the presence of L-NAME

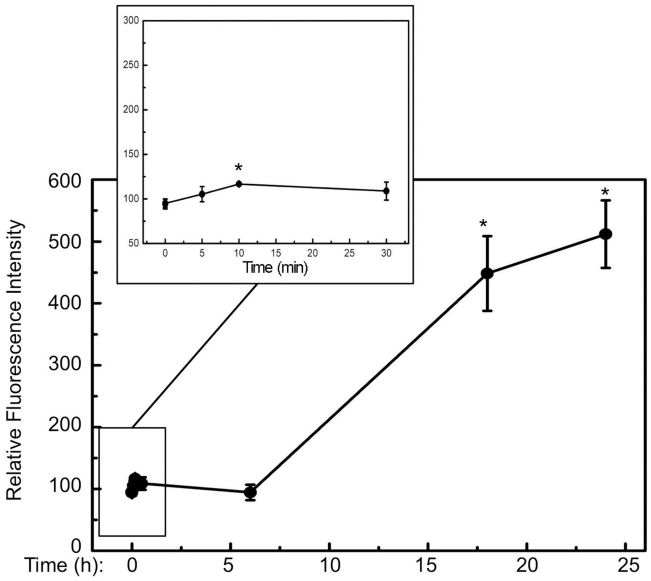

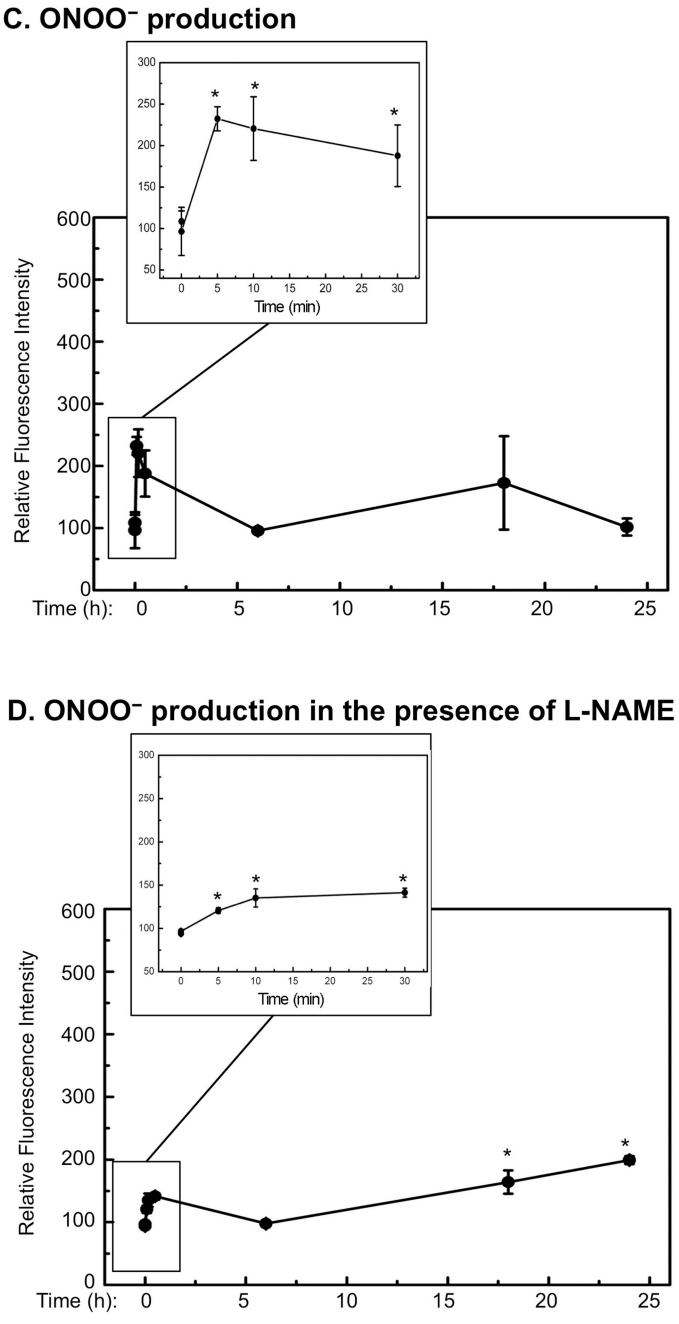

Fig. 2.

Quantitative analysis of NO• and $ONOO^-$ after UVB-irradiation. HaCaT cells were irradiated with UVB (75 mJ/cm^2) in the absence or presence of L-NAME. At the indicated time-points post-UVB-irradiation, the cells were stained with DAF-2DA or DAR. The fluorescence intensity was then measured and corrected with respect to cell viability. The fluorescence intensities of (A) NO• in the absence of L-NAME; (B) NO• in the presence of L-NAME; (C) $ONOO^-$ in the absence of L-NAME; and (D) $ONOO^-$ in the presence of L-NAME were shown. The error bars present the standard deviations of 3 independent experiments. *: $p<0.05$ vs. control.

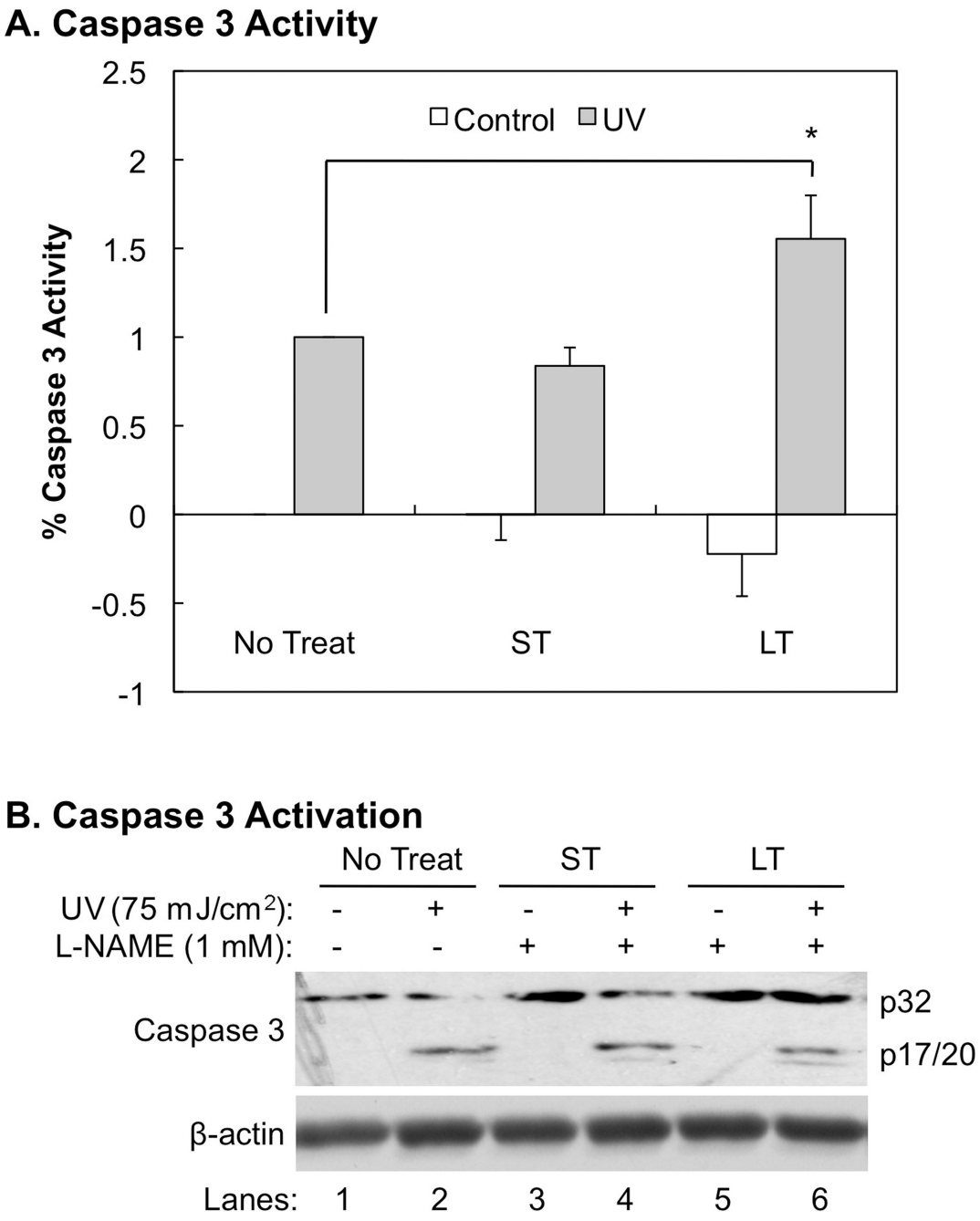

Fig. 3.

The effects of inhibiting cNOSs on UVB-induced caspase-3 activity and cleavage. The cells were treated with L-NAME for a short (ST, 0.5 h post-UVB) or longer period (LT, 18 h post-UVB) of time as described in “Methods”. (A) Caspase 3 activity was determined by using a fluorescent substrate, FAM-DEVD-FMK, of caspase 3. The fluorescence intensity was normalized with the caspase 3 activity in the untreated sample (No Treat). The error bars present the standard deviations of 3 independent experiments. *: $p<0.05$ vs. control. (B) Western blot analysis of caspase 3 cleavage.

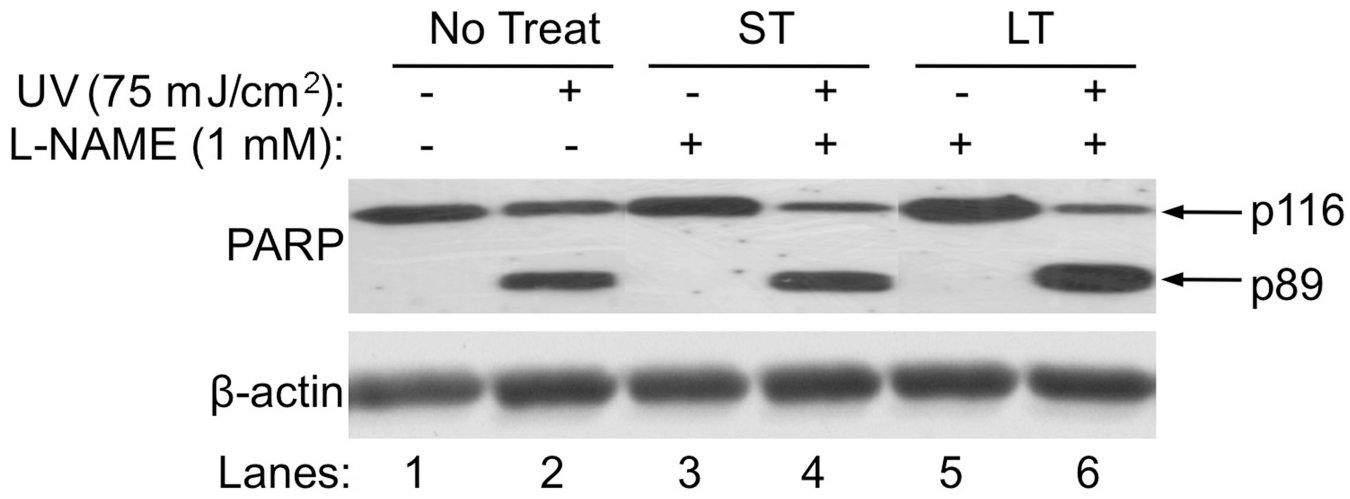

Fig. 4.

The effects of inhibiting cNOSs on UVB-induced PARP cleavage. UVB-induced PARP cleavage in HaCaT cells that were not treated or treated with L-NAME was determined by western blot analysis. No Treat: without L-NAME treatment. ST: treated with L-NAME for a short of time (0.5 h post-UVB). LT: treated with L-NAME for a longer period of time (18 h post-UVB).

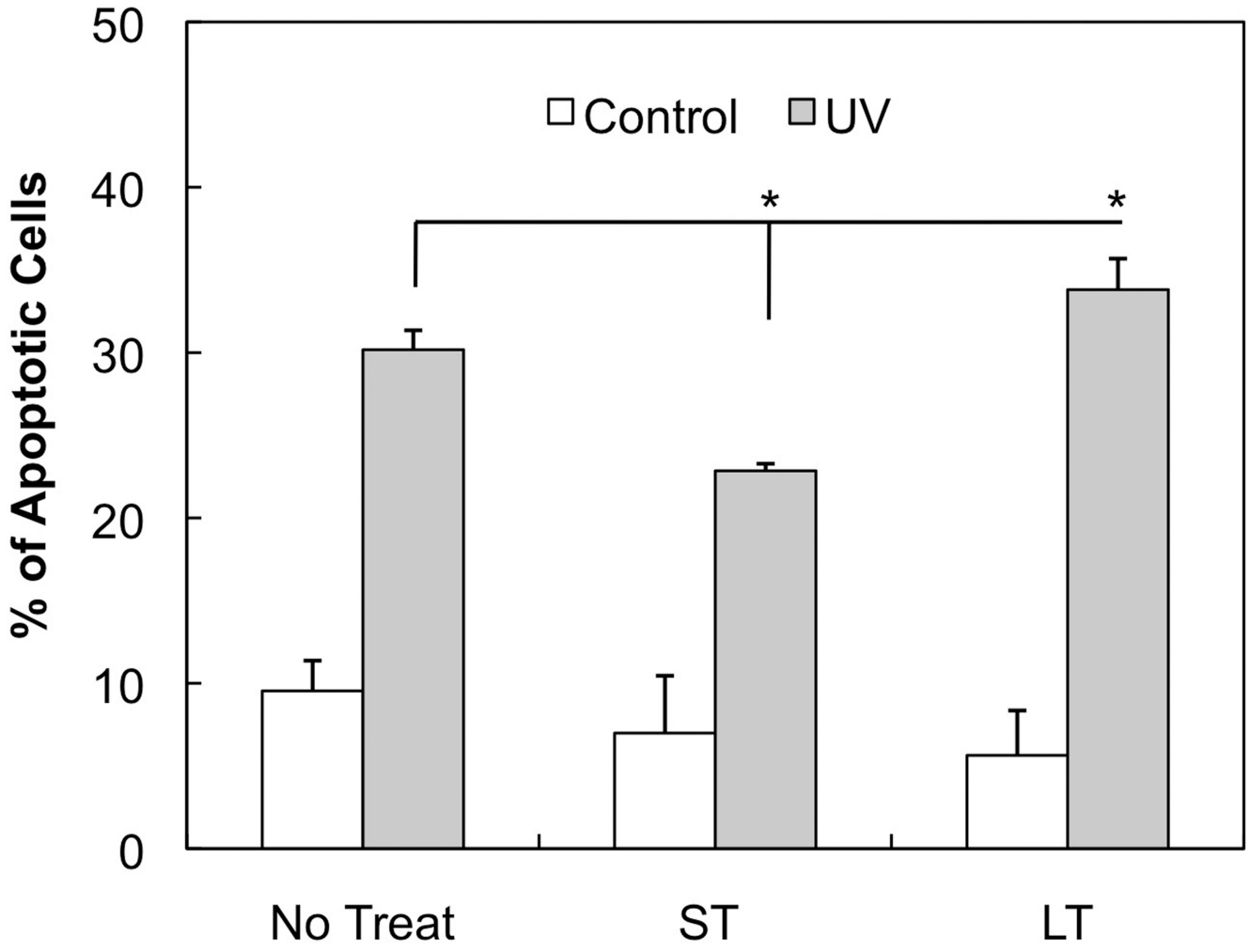

Fig. 5.

The effects of inhibiting cNOSs on UVB-induced apoptosis. HaCaT cells were UVB irradiated and then were not treated (No Treat) or treated with L-NAME for a short (ST, 0.5 h post-UVB) or longer period (LT, 18 h post-UVB) of time. The cells were then double stained with ANX5-FITC/PI at 18 h post-UVB and apoptosis was analyzed by flow cytometry. The error bars present the standard deviations of 3 independent experiments. *: $p<0.05$ vs. control.

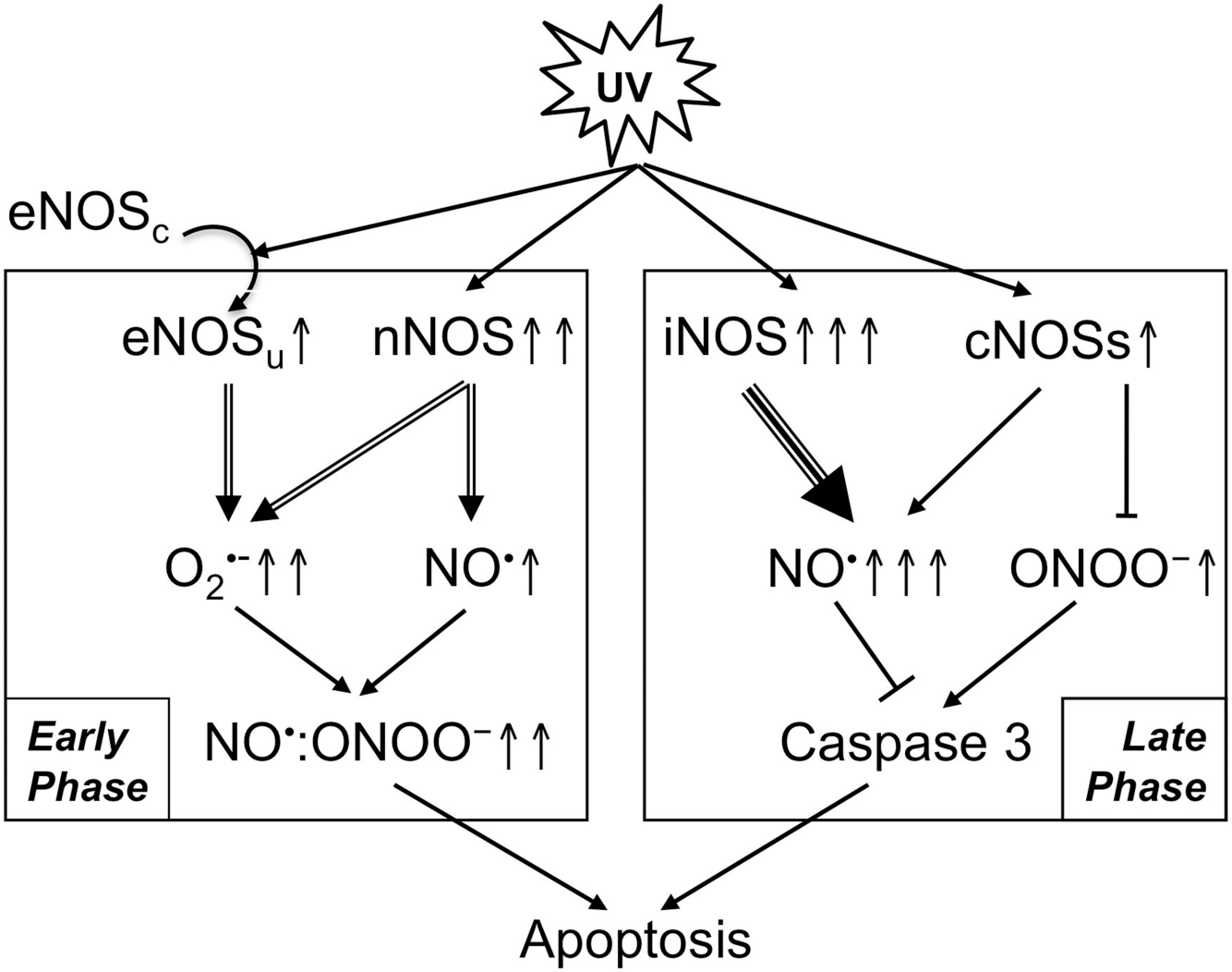

Fig. 6.
Proposed NOSs signaling network after UVB-irradiation.

Table I

Relative amount of $NO^{\bullet}$ and $ONOO^{-}$ in the presence or absence of L-NAME after UVB-irradiation

The data is normalized with $NO^{\bullet}$ or $ONOO^{-}$ respectively produced in HaCaT cells without any treatment. Means±SE of 3 independent experiments were shown.

	Time	0	5 min	10 min	30 min	6 h	18 h	24 h
$NO^{\bullet}$	UV alone	1.3±0.4	1.4±0.7	2.7±0.3	1.5±0.5	1.5±0.3	10.1±0.3	9.9±0.3
	UV+L-NAME	1.7±0.1	1.8±0.1	2.0±0	1.9±0.2	1.6±0.2	7.8±1.1	8.9±0.9
$ONOO^{-}$	UV alone	0.9±0.3	2.1±0.1	2.0±0.4	1.7±0.3	0.9±0	1.6±0.7	0.9±0.1
	UV+L-NAME	0.9±0	1.1±0.1	1.2±0.1	1.3±0	0.9±0	1.5±0.2	1.8±0.1
$NO^{\bullet}$/ $ONOO^{-}$	UV alone	1.4	0.7	1.4	0.9	1.7	6.3	11.0
	UV+L-NAME	1.9	1.6	1.7	1.5	1.8	5.2	4.9